Laser Chem. 1983, Vol. 3, pp. 29–47
0278-6273/83/0306-0029$12.00/0

Printed in Great Britain

Multiphoton Ionization Mass Spectrometric (MPIMS) Study of Phenol: Mechanism of Ionic Fragment Formation†

R. S. PANDOLFI,‡ D. A. GOBELI, JONATHAN LURIE§ and M. A. EL-SAYED

Department of Chemistry, University of California, Los Angeles, California 90024

Time of flight (TOF) mass spectrometry is used in conjunction with a variable repelling voltage technique to elucidate the mechanism by which phenol ionizes and dissociates under 266 nm pulsed laser irradiation in combination with a 532 nm or 355 nm pulsed laser. The results suggest that, like benzene, the molecular ion is the predominant precursor of all ionic species generated in the process. Predominance of $C_5H_X^+$ species at relatively low powers confirms the presence of a low energy dissociation channel involving the elimination of CO. The use of a second laser at 532 nm is found to selectively destroy the $C_5H_X^+$ (as compared to the parent ion) species. The parent ion is found to be protected from the radiation of the second laser pulse at 532 nm but not at 355 nm if the second laser pulse is delayed by 50 ns. This is explained in terms of relaxation within the parent ion energy levels, the location of a low energy dissociation channel and the wavelengths of the lasers used. The main aspects of the fragmentation pattern are discussed in terms of the statistical theory of Rebentrost and Ben-Shaul.

Unlike electron impact mass spectrometry, which commonly uses either quasiequilibrium or RRKM theory to interpret fragmentation patterns,[1] there appears to be no unifying theory which predicts multiphoton ionization-dissociation (MPID) mass spectral results. Instead, three mechanisms have been suggested which attempt to

† Part of this work was used in partial fulfillment of the Ph.D Degree of RSP and DAG.

‡ Present address: Department of Physics, Argonne National Laboratory, Argonne, Ill. 60439.

§ Present address: Air Force Geophysics Laboratory, Hanscom Air Force Base, MA 01731.

explain MPID mass spectra.[1–7] Each mechanism tends to be more applicable in certain instances, depending upon the system under consideration and the frequency of excitation used.

In the first mechanism, the molecular ion is the precursor of all other ions.[2] After the molecular ion is generated, it absorbs further photons to fragment into smaller ions which in turn absorb more photons etc. This is commonly referred to as the ionic ladder climbing mechanism and has been cited in numerous instances.[2,5,6] In the second mechanism, the molecule fragments through low energy dissociation channels before ionization occurs.[7] Therefore no common precursor intermediate exists for all observed ionic species. This mechanism has often been used to discuss the fragmentation behavior of organometallic systems.[8,9] In the third mechanism the neutral molecule absorbs many more photons than are necessary to reach the lowest ionization potential before it does so.[4] When it does, all observed species are simultaneously generated in one step and the entropic theory has been conveniently applied.[10]

Phenol has been the subject of numerous recent mass spectrometric investigations.[11–14] Among the topics discussed has been the purported isomerization of the phenol radical cation to another structure prior to fragmentation. Several structures have been suggested. The sources of excitation used in all these reports include electron impact, field ionization collision induced dissociation and electron impact collision induced dissociation.

In this paper we have two sections. In the first, experimental results on the effect of laser power, laser wavelength, and repelling voltage using one or two pulsed lasers upon the fragmentation pattern of phenol are presented. In addition, results are given for the two-color experiment on the effect of the decay between the pulses. The results elucidate whether ionization or fragmentation is the primary process in the laser induced MPID of phenol.

As with other aromatic systems such as benzene,[2] benzene-d_6,[15] and aniline,[16] phenol is found to fragment via the ionic ladder climbing mechanism under 266 nm excitation. An interesting effect of the delay is observed and discussed.

In the second section of the paper, the Rebentrost–Ben-Shaul theoretical mechanism[17] is used to qualitatively discuss the main results obtained.

1. EXPERIMENTAL STUDIES

Experimental

The apparatus consists of a time-of-flight mass spectrometer designed for use with a multiphoton ionization source. More details of the apparatus are given elsewhere.[15]

The fourth harmonic (266 nm) of a Quanta-Ray DCR Nd:YAG laser is focussed with a 13 cm quartz lens into the ionization region of the mass spectrometer. The second (532 nm) or third (355 nm) harmonic is cofocussed through another 13 cm quartz lens into the ionization region along the same optical path as the 266 nm pulse but with different direction of propagation. Experiments have been carried out with the second and fourth harmonics simultaneously, with optical delays of 6, 25, and 50 ns. Generally, the 266 nm fourth harmonic was generated with approximate energy of 0.1 mJ/pulse; the 532 nm second harmonic, and the 355 nm third harmonic were kept at approximately 5 mJ/pulse.

The repelling potential method used to elucidate the mechanism of multiphoton ionization dissociation is described in detail elsewhere.[15] Briefly, two laser pulses separated in time by up to 50 ns are cofocussed at the entrance of a time-of-flight mass spectrometer. By varying the acceleration potential, it is possible to expose ions created by the first pulse to varying amounts of the second pulse. It is therefore possible to observe the evolution of ion signal due to fragmentation caused by the second pulse.

Results and discussion

Below we summarize and discuss the different experiments.

A. *The results of the 266 nm experiment*

1) Except for very low laser powers, significant amounts of $C_6H_6O^+$ and $C_5H_X^+$ are observed simultaneously (see bottom spectrum in Figure 1). This is in contrast to benzene[2] and benzene-d_6 [15] where it is possible to produce exclusively the molecular ion in large quantities at moderate laser powers. This can be explained by the fact that the formation of $C_4H_X^+$, the lowest energy fragment of fewer than six

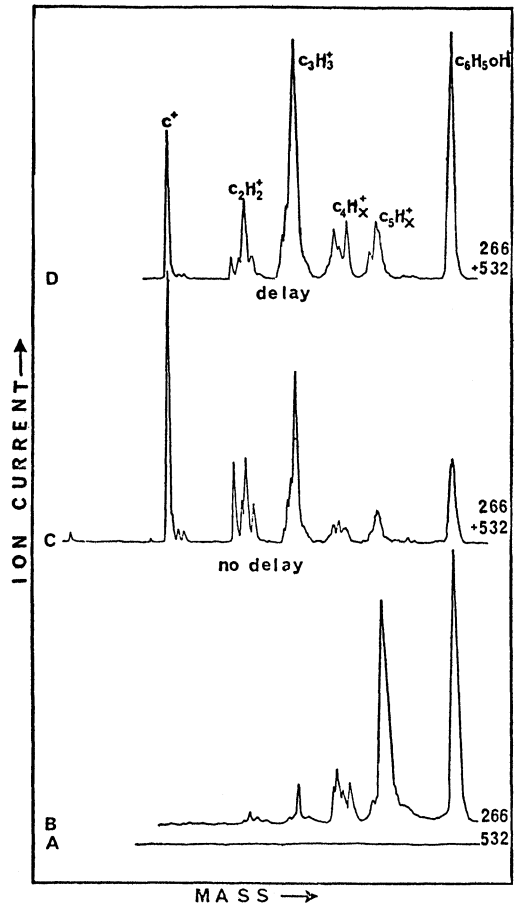

FIGURE 1 The effect of delay in two color experiments on the fragmentation pattern of phenol: (a) 532 nm alone showing that at the power used; ion formation is not possible by multiphoton processes. (b) 266 nm alone results in ion formation. (c) 266 nm + 532 nm with no delay leading to parent destruction. (d) 266 nm + 532 nm with 50 ns delay showing a relative protection of the parent.

carbon atoms from benzene, requires an excess of 5 eV above the ionization continuum (i.e., a two photon process using 266 nm photons)[18] whereas the formation of $C_5H_6^+$ fragments from phenol requires only 3 eV of energy (one 266 nm photon) above the ionization continuum.[13] Thus, the difference in rate processes requiring

one- and two-photon absorption might account for this observation.

2) Figure 2 shows that as the laser power increases, the parent ion yield relative to the total ion current decreases, while the $C_5H_6^+$ and $C_3H_3^+$ yields increase. This suggests that the $C_5H_6^+$ species is derived from the molecular ion by the absorption of radiation. This together with the fact that it is formed with a high yield might suggest that the $C_5H_X^+$ species is mostly $C_5H_6^+$.

B. *Two color experiments*

1. The effect of the delay (Figure 1).

The 532 nm laser pulse alone does not fragment the phenol molecular ion at the powers used in our experiments. However, as shown in Figure 1, in the presence of the 266 nm laser radiation, both the parent ion and the $C_5H_X^+$ ions are found to decrease while the $C_3H_X^+$, $C_2H_X^+$, and CH_X^+ yields increase. This suggests that both the parent ion and the $C_5H_X^+$ fragment formed by the 266 nm radiation absorb the 532 nm radiation to yield smaller ions. If the 532 nm radiation is delayed from the 266 nm pulse, it becomes inefficient at destroying the parent ion but continues to fragment the $C_5H_X^+$ species (Figure 1d). This might suggest that fragmentation of the parent ion by the green laser pulse is possible from an excited level of the ion. The delay between the two laser pulses allows for the relaxation of ions to take place from this level to other levels or configurations from which the absorption of the green laser radiation has a much reduced one-photon transition probability.

Phenol has an intense absorption around 266 nm (4.66 eV). Because of this, and the relatively low value of its ionization potential (8.37 eV as determined from its photoelectron spectrum)[19] it is possible to reach the first excited electronic state of the phenol radical cation with a one-photon resonant, two-photon ionization process with the 266 nm radiation. Figure 3 shows an energy level diagram of phenol and its molecular ion. According to this diagram, two 266 nm photons excite phenol to the $^2A_2$ level of the molecular ion. One green photon can energetically dissociate the molecular ion from this level to give $C_5H_6^+$ and CO. If however the $^2A_2$ level of the parent ion could relax radiatively to the ground vibrational state of the $^2B_1$ level of the ion or nonradiatively to an excited vibrational level of

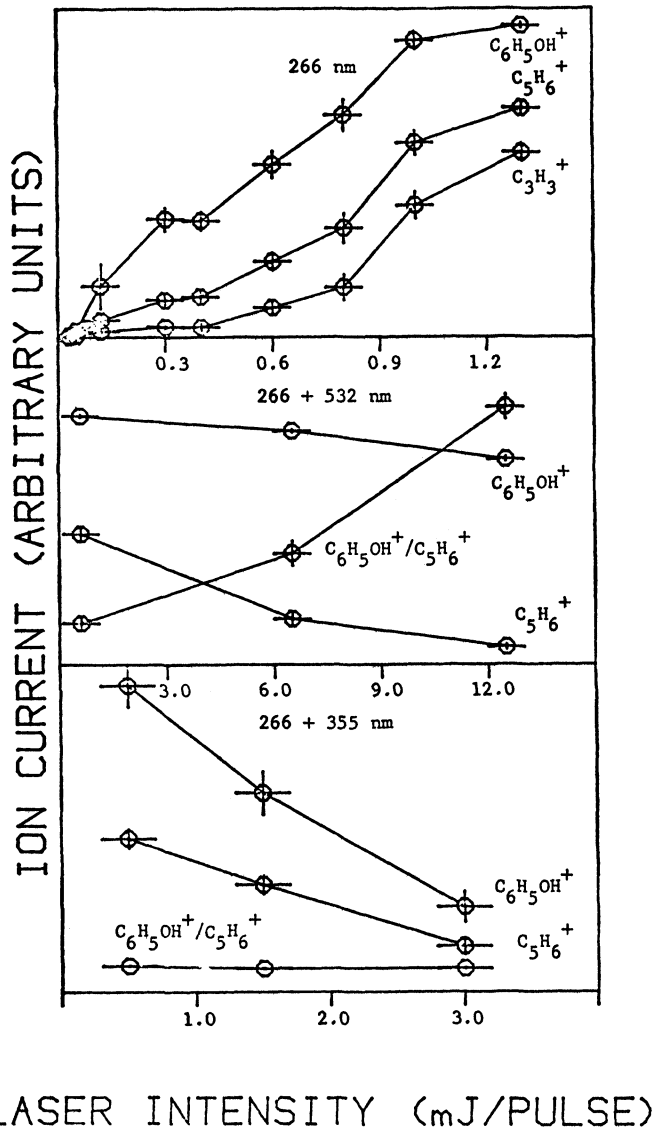

FIGURE 2 The effect of laser power on the fragmentation pattern.

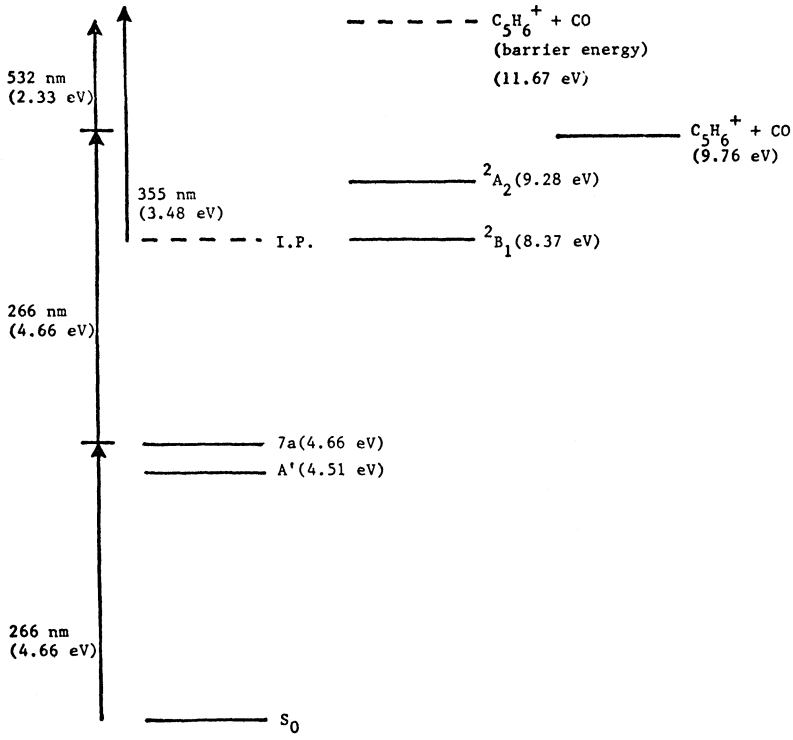

FIGURE 3 Partial energy level diagram of phenol and its cation together with the lowest energy channel-elimination of CO from the phenol cation. The energy of the photons of the different lasers used are shown with vertical arrows.

the $^2B_1$ electronic state, a one photon absorption at 532 nm is either energetically insufficient to overcome the barrier to dissociation, or possesses a low absorption coefficient for the excited vibrational levels of the $^2B_1$ state. One photon of the 355 nm radiation is capable of dissociating the ground vibrational state of the ion. Thus, if relaxation occurs to any of the vibrational levels of the ground electronic state, the ion might still have sufficient absorption coefficient that would make this wavelength efficient in fragmenting the molecular ion, even if it is delayed. This is shown in Figure 4.

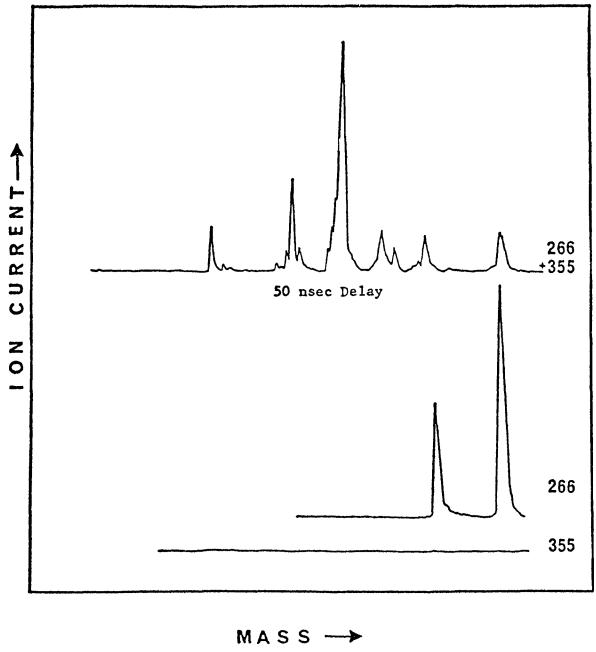

FIGURE 4 The effect of the delay of the 355 nm laser on the two color (266+355 nm) fragmentation pattern. Unlike the 532 nm laser, the effect of delaying the 355 nm laser does not protect the parent ion destruction.

2. The contribution of neutrals.

Figure 5 shows that like benzene, further fragmentation with the 50 ns delayed 532 nm laser is found to diminish as the repelling voltage is increased (thus removing the parent and the $C_5H_X^+$ ions formed from the first laser out of the focus of the delayed laser beam). This suggests that the contribution of neutral fragments formed from the first laser pulse to the formation of the small ionic fragments with the 532 nm pulse is not significant.

3. Power dependence.

The power dependence of the 532 nm and 355 nm radiation delayed for 50 ns from the 266 nm ionizing pulse is shown in Figure 2. The results are consistent with the above discussion. At the powers used

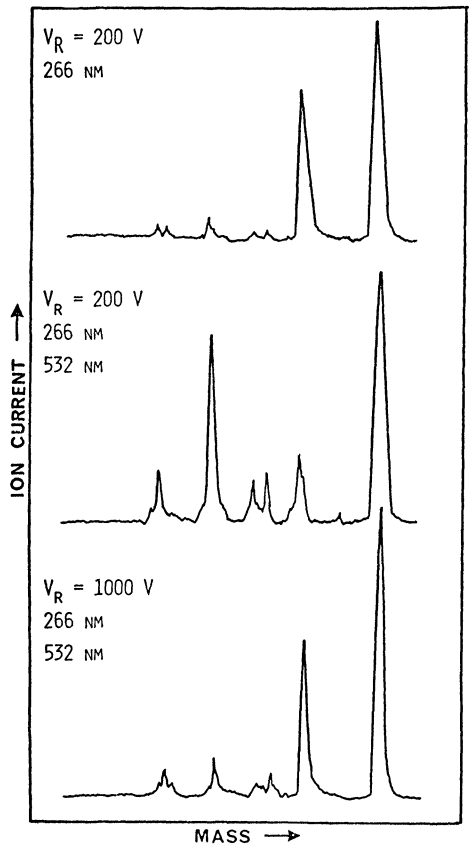

FIGURE 5 The effect of increasing the repelling potential in the 50 ns delayed two color (266 + 532 nm) experiment. The destruction of the primary pattern (formed from Hthe 266 nm radiation) with the 532 nm laser is found to be eliminated at high repelling voltage. This suggests a lack of neutral contribution to the ionic pattern from the 532 nm laser, as observed for benzene, aniline, and benzene-d_6.

of the 266 nm laser, the yield of the parent ion seems to be insensitive to the 532 nm power, but generally decreases with increasing the 355 nm power. The $C_5H_X^+$ yields decrease continuously with the 532 nm power but increase first (due to the destruction of the parent ion), then decrease (due to its own destruction) as the power of the 355 nm radiation increases.

General observations and possible conclusions

The results of the repelling voltage study (Figure 5) are consistent with the ladder climbing mechanism. That is, the molecular ion is the precursor of all other fragments. In contrast to similar experiments performed on benzene however, significant amounts of the daughter ion ($C_5H_X^+$) are usually present. This is indicative of a low energy pathway (requiring in the case of $C_5H_X^+$ one additional 532 nm photon) from the parent to daughter ion.

After delays of 6, 25, and 50 ns, the parent ion is unaffected by the 532 nm radiation. We interpret this to mean that, during such time, the initially prepared first excited state of that ion decays to the ground electronic manifold by nonradiative processes from whose levels the absorption of 532 nm radiation has a very small one-photon transition probability. When the laser pulses are made coincident in time, absorption of the 532 nm photons may take place from the excited electronic level of the phenol radical cation leading to further climbing of the ionic ladder and leading to further dissociation.

When the 532 nm pulse was replaced with a 355 nm pulse, it becomes possible to dissociate the molecular ion directly from its ground electronic state, thus causing attenuation of the molecular ion signal even after delays are introduced.

In both delayed and non-delayed experiments, the $C_5H_6^+$ radical cation absorbs at 532 nm and at 355 nm as is exemplified by its destruction at these wavelengths. Obviously, the extent and the specificity of ion destruction is sensitive to the power of the laser pulse, as well as its wavelength. This might open the field of determining the absorption spectrum of different ions by positive ion destruction spectroscopy.

The molecular ion of phenol displays a wavelength dependence to the second laser pulse. It is also sensitive to the delay between the first and the second pulse. When that pulse was the 532 nm second harmonic of the YAG, no destruction of the ion was observed with delay. On the other hand, delaying the 355 nm (third harmonic of the YAG) pulse is found to result in partial destruction of the molecular ion. As mentioned earlier, we interpret this as signifying that the 355 nm pulse might still be absorbed even if the delay causes a relaxation to any of the vibrational levels of the $^2B_1$ electronic state. This might not be the case for the absorption of the 532 nm laser

radiation. The observed lack of parent ion destruction at this wavelength if it is delayed from the ionizing pulse could be explained in terms of relaxation to excited vibrational levels of the $^2B_1$ state from which absorption at this wavelength has a low probability. Therefore, at moderate laser powers no significant fragmentation is observed.

In both delayed and non-delayed experiments, the $C_3H_X^+$ fragment cation is the predominant product of the destruction of $C_5H_X^+$ under our experimental conditions of moderate laser power. This suggests that the second step in the dissociation of the phenol radical cation involves the elimination of acetylene (C_2H_2). Under conditions of high laser power for the second laser pulse, C^+ is the predominant species observed.

Conclusion

The multiphoton ionization fragmentation mechanism of phenol arises from ionic ladder climbing. There are indications that the elimination of CO is the predominating first step in the fragmentation of the molecular ion. The resulting $C_5H_X^+$ fragment is selectively destroyed (as compared to the parent ion) by exposure to a second laser with 532 nm photons, delayed on the *ns* time scale from the initial ionizing laser pulse. This might suggest a means of determining the spectra of this positive ion by destruction spectroscopy.

The fragmentation of the parent ion by a second laser pulse is found to be diminished if a delay of 50 ns is used for the 532 nm pulse but not for the 355 nm pulse. An explanation invoking relaxation amongst the vibronic energy levels of the ion and a possible change in absorption cross section and a low energy dissociation channel yielding the $C_5H_X^+$ species is given.

2. MULTIPHOTON IONIZATION-DISSOCIATION OF PHENOL: A FURTHER TEST OF STATISTICAL THEORY

Although many multiphoton ionization-dissociation experiments have been carried out, relatively little theoretical work has been attempted to better elucidate this fascinating observation in experimental chemical physics. The approach developed by Rebentrost and

Ben-Shaul[15] utilizes statistical methods to explain the multiphoton dissociation of benzene ion. Many different ionic species are produced in this experiment, necessitating the adoption of a simplified density of product-states treatment in the statistical calculations. Although this model reproduced well the benzene ion multiphoton-induced mass spectra, this system is probably not the most sensitive test of this model, owing to the large number of dissociation pathways, which might tend to wash out relatively small differences between statistical and non-statistical processes.

A better test of the model might be the phenol ion. The multiphoton ionization mass spectra of this species are simpler, even at high laser power, than the benzene spectra. This might be because there are several fragmentation pathways for phenol ion and its primary daughter fragment, $C_5H_6^+$, which lie at relatively low energy. These are:

$$C_6H_6O^+ \rightarrow C_5H_6^+ + CO \qquad \Delta H = 32.7 \text{ kcal/mole}$$

$$C_5H_6^+ \rightarrow C_3H_3^+ + C_2H_3 \qquad \Delta H = 65 \text{ kcal/mole}$$

$$C_5H_6^+ \rightarrow C_2H_2^+ + C_3H_4 \qquad \Delta H = 72.3 \text{ kcal/mole}$$

Therefore, the potential exists for a sensitive test of the Rebentrost–Ben-Shaul method. In this section, the results of statistical calculations for this dissociation system are presented, and compared with experimental mass spectra of the phenol ion, given in Section 1.

Equations and data for calculations

For an ion i^+ fragmenting to the species $j^+ + n$, the Rebentrost–Ben-Shaul model gives the unnormalized fragmentation probability[17] as:

$$P_{ij}(E_i, E_j) = C_t \mu_{jn}^{3/2} \alpha_{ij} g_j g_n Q_j Q_n \frac{(E_j + a_j E_{0j})^{S_j + r_j/2 - 1} (E_n + a_n E_{0n})^{S_n + r_n/2 + 1/2}}{\Gamma(S_j + r_j/2) \prod_{S_j} h\nu_j \Gamma(S_n + r_n/2 + 3/2) \prod_{S_n} h\nu_n}$$

where C_t is a constant with units of $(\text{momentum})^{-3}$, μ_{jn} is the reduced mass of the $j^+ - n$ pair, α_{ij} is the path degeneracy, g_j and g_n are electronic degeneracies, Q_j and Q_n are rotational factors given by:

$$Q_j = \frac{1}{\sigma_j} (8\pi^2/\hbar^2)^{r_j/2} \pi^{1/2} \prod_{r_j} I_j^{1/2}$$

E_j, E_i and E_n are energies of the respective species, related by the balance

$$E_i - \Delta H_{i \to j} = E_j + E_n$$

a and r are the number of vibrational and rotational degrees of freedom, the $a_j E_{0j}$ terms represent zero-point vibrational energy (taken as zero in these calculations) and $\prod h\nu$ represents the product of all vibrational frequencies of species j^+ and n. This expression is the internal energy distribution ion j^+.

When this expression is integrated over E_j, the total dissociation probability of $i^- \rightarrow j^+$ is obtained. These integrals are of the form:

$$\int_0^a dx\, x^{n/2}(a-x)^{m/2} = a^{n/2+m/2+1} \frac{\Gamma(n/2+1)\Gamma(m/2+1)}{\Gamma(n/2+m/2+2)}$$

When this entire calculation is completed for all processes $i^+ \rightarrow j^+$, $i^+ \rightarrow k^+$, $i^+ \rightarrow 1^+$ etc, for a given E_i, branching ratios may then be directly taken.

The following dissociation processes were investigated. The data necessary to do calculations on these species are listed in Tables I and II.

Results

A. *$C_6H_6O^+$ dissociation* The process:

$$C_6H_6O^+ \rightarrow C_5H_6^+ + CO$$

has a ΔH of 32.7 kcal/mol. All other dissociation processes lie considerably higher in energy. Indeed, the spectrum in Figure 5 (top) shows only C_6 and C_5 ions, probably making this the sole dissociation channel for $C_6H_6O^+$ in this experiment. However, some of the C_4 ions appearing in the spectrum in Figure 1b might actually be acrolein (CH_2CHCHO) ions. Therefore, a rough calculation was performed for the process:

$$C_6H_6O^+ \longrightarrow C_3H_4O^+ + C_3H_2 \qquad \Delta H = 162 \pm 20\% \text{ kcal/mol}$$

This process becomes roughly equal in probability to process (1) for $E_i = 600$ kcal/mol, or six 266 nm photons, an unreasonably large energy deposition.

TABLE I
Dissociation processes investigated in this study[20]

$C_6H_6O^+ \longrightarrow C_5H_6^+ + CO$	$\Delta H = 32.7$ kcal/mol
$\longrightarrow C_3H_4O^+ + C_3H_2$ $(H_2C{=}CH{-}CHO^+)$	162 ± 20%
$C_5H_6^+ \longrightarrow C_4H_6^+ + C$ $(H_2C{=}CHCH{=}CH_2^+)$	177.3
$\longrightarrow C_4H_5^+ + CH$	153.4
$\longrightarrow C_4H_4^+ + CH_2$ (Δ^+) (linear)	142.7
$\longrightarrow C_4H_3^+ + CH_3$	111.2
$\longrightarrow C_4H_2^+ + CH_4$ $(H{-}C{\equiv}C{-}C{\equiv}C{-}H^+)$ (linear)	100.1
$\longrightarrow C_3H_3^+ + C_2H_3$ (Δ^+) ( )	65
$\longrightarrow C_2H_2^+ + C_3H_4$ (linear) $(H_3C{-}C{\equiv}CH)$	72.3

TABLE II
Necessary data for dissociation species[20]

	σ	g	I (cm^{-1})	$(\prod h\nu)^{1/s}$ (cm^{-1})
$C_5H_6^+$	2	2	$\sqrt{I_aI_BI_c} = 0.118$	1230
$C_4H_6^+$	1	2	1.37, 0.1413, 0.1413	1180
$C_4H_5^+$	1	2	1.37, 0.2, 0.2	1150
$C_4H_4^+$	2	2	1.00, 0.15, 0.13	1143
$C_4H_3^+$	2	1	9.5, 0.15, 0.15	1078
$C_4H_2^+$	4	6	0.14, 0.14	812
$C_3H_3^+$	6	1	1.0, 1.0, 0.5	1252
$C_2H_2^+$	2	4	1.15, 1.15	1225
$C_3H_4O^+$	1	2	$\sqrt{I_aI_BI_c} = 0.186$	1130
C_3H_4	3	2	5.21, 0.285, 0.285	1238
C_3H_2	2	2	$\sqrt{I_aI_BI_c} = 0.25$	1211
C_2H_3	2	2	9.0, 1.06, 0.95	1586
CH_4	12	1	5.2412, 5.2412, 5.2412	1957
CH_3	6	2	9.6, 4.8, 4.8	2072
CH_2	2	3	7.9, 7.9	2049
CH	1	4	14.5, 14.5	2858
CO	1	1	1.93, 1.93	2170
C	1	9	—	—

B. *$C_5H_6^+$ Dissociation to C_4^+ Species* For $E_i = 214$ kcal/mol (four 532 nm photons), the probabilities for each of these dissociation processes increases as the ΔH for the processes decrease, which might be expected. However, none of these C_4 species appears for certain in the experimental spectra. Even for $E_i = 250$ kcal/mol, the probability of the *most probable* $C_5^+ \rightarrow C_4^+$ process is calculated to be 200–300 times smaller than the *least probable* $C_5^+ \rightarrow C_3^+ + C_2$ process. Higher levels of energy deposition are improbable. Therefore, $C_5^+ \rightarrow C_4^+$ processes appear to be unimportant in this experiment.

C. *$C_5^+ \rightarrow C_3^+ + C_2$* The species $C_3H_3^+$ and $C_2H_2^+$ appear prominently in the experimental mass spectra. While the $C_3H_3^+/C_2H_2^+$ ratio varies to some degree, probably because of differing laser powers between the spectra, the value is around four in Figure 1c. Accordingly, calculations were performed for varying E_i. The value of E_i producing a branching ratio of four was found to be 190–195 kcal/mol (Figure 6).

The internal energy distribution for $C_5H_6^+$ formed from phenol ion is plotted in Figure 7 for total absorbed photon energy of 3×266 nm. $E(p_{max})$ is at 88.5 kcal/mol.

Discussion

The statistical theory calculations correctly predict the relative absence of ions other than $C_6H_6O^+$ and $C_5H_6^+$ at low laser powers. Some 266 nm single-beam spectra show a few other ions at lower masses, but this is most probably due to $C_5H_6^+$ dissociation. Of course, this is not a sensitive test of the theory. Since the threshold for $C_6H_6O^+ \rightarrow C_5H_6^+ + CO$ is so much lower (at least 70 kcal/mol) than the other $C_6H_6O^+$ dissociation processes, one might expect this channel to be the only one operative even if statistical theory did not apply here. In all probability, it does not apply, since CO abstraction from $C_6H_6O^+$ is not a simple bond scission.

The statistical calculations also are in accord with the apparent absence of a series of $C_4H_n^+$ species arising from $C_5H_6^+$. On the other hand, it is not possible to explain with this theory the dual peaks in the C_4 region observed in the experimental mass spectra. In order to understand the C_4 region better, it is necessary to accurately assign

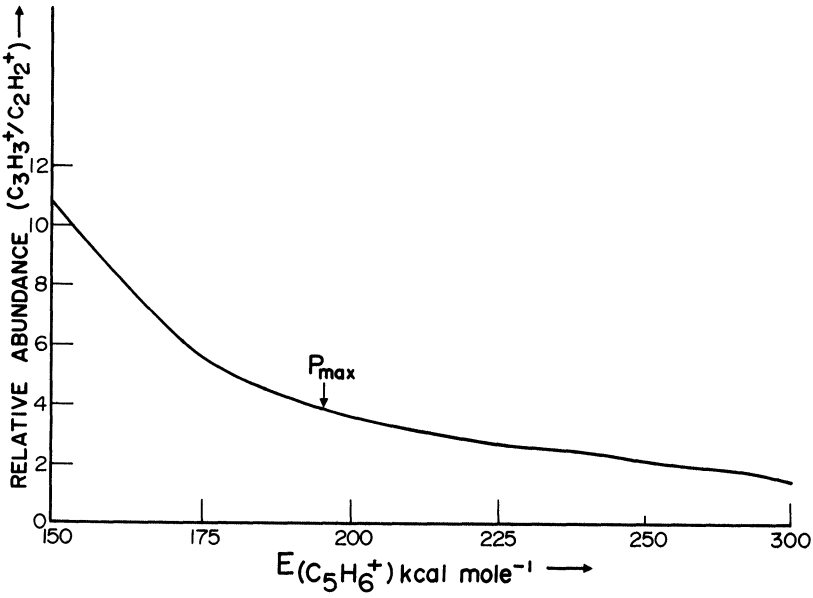

FIGURE 6 The $(C_3H_3^+)/(C_2H_2^+)$ ionic ratio as a function of the internal energy of $C_5H_6^+$. The observed ratio in Figure 1c (~4), requires ~190 kcal/mol (i.e., by penol absorbing 3 × 266 nm photons to form $C_5H_6^+$ followed by two 532 nm photons to create these two ions).

the masses of these two peaks. In any event, it appears that a non-statistical constraint operates to produce this pair of peaks.

However, the statistical theory proves very useful for explaining the $C_3H_3^+/C_2H_2^+$ ratio produced from $C_5H_6^+$ dissociation. A consideration of the photon usage in the 266 nm single-beam experiment is enlightening here. Two 266 nm photons supply 9.32 eV. The ionization potential of phenol is 8.37 eV. This leaves 0.95 eV or 22 kcal/mol to cause dissociation of $C_6H_6O^+$, which is less than the 32.7 kcal required for the $C_5H_6^+ + CO$ channel. Therefore, further 266 nm photon absorption is required to cause dissociation. One further 266 nm photon supplies 107 kcal/mol. Then the maximum possible energy which could be present in $C_5H_6^+$ is $107 + 22 - 32.7 = 96.3$ kcal/mol. The energy distribution of $C_5H_6^+$ calculated from the statistical theory shows $E(p_{max}) = 88.5$ kcal/mol, with >90% of the $C_5H_6^+$ ions having higher energy than the threshold for $C_5H_6^+ \rightarrow C_2H_2^+ + C_3H_4$, $\Delta H = 72.3$ kcal/mol. However, most $C_5H_6^+$

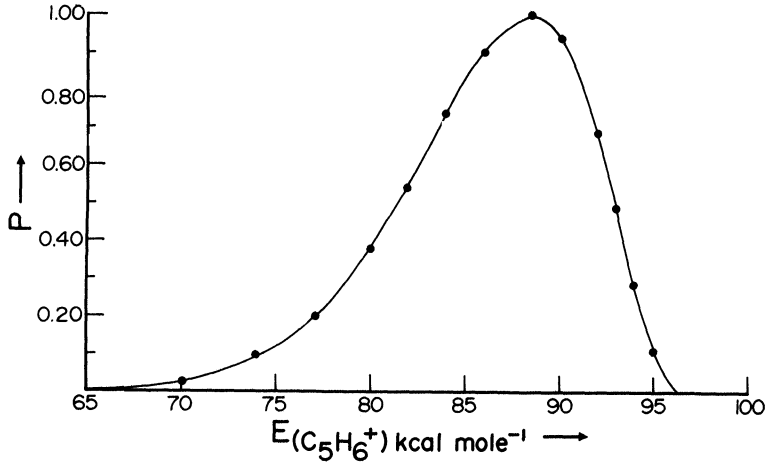

FIGURE 7 The internal energy distribution for the $C_5H_6^+$ formed from phenol ion as a function of the total absorbed energy of 3×266 nm photons. The figure shows that the statistical theory predicts that the most probable internal energy of $C_5H_6^+$ is 88.5 kcal/mol.

ions are not dissociated to smaller species, even though the threshold energy has been exceeded. Clearly, most $C_5H_6^+$ ions are metastable on a time scale of this experiment (1 μs).

However, a total energy deposition of 3×266 nm photons is insufficient to create the observed $C_3H_3^+/C_2H_2^+$ branching ratio of four in the calculation. Approximately 100 kcal/mol (1×266 nm, 2×532 nm) additional energy above $E(p_{max}) = 88.5$ kcal/mol is necessary. Therefore, we believe that for those dual-beam spectra with a $C_3H_3^+/C_2H_2^+$ ratio of four, three 266 nm photons are absorbed to create CO and $C_5H_6^+$ which then absorbs two additional green photons to create $C_3H_3^+$ and $C_2H_2^+$. In this case, the statistical theory provides a natural and reasonable explanation for the experimental mass spectra, although this does not constitute absolute proof of its validity.

Summary

There appear to be certain aspects of multiphoton dissociation of $C_6H_6O^+$ which may be explained by the Rebentrost–Ben-Shaul

theory. Specifically, the theory explains the $C_3H_3^+/C_2H_2^+$ branching ratio arising from $C_5H_6^+$ dissociation. On the other hand, it gives little information about the initial dissociation of $C_6H_6O^+$, and appears to be inconsistent with the experimental results in the C_4 region. In any event, this is a promising system on which to carry out experiments in order to establish whether this theory works in this case, since the mass spectra are relatively simple except at very high powers, making it easier to reject certain dissociation pathways. This research is now in progress.[21]

Acknowledgement

We wish to thank the National Science Foundation for their financial support.

References

1. J. C. Lorquet, *Org. Mass Spectrom.* **16,** 469, (1981).
2. U. Boesl, J. J. Neusser and E. W. Schlag, *J. Chem. Phys.* **72,** 4327, (1980).
3. V. S. Antonov and V. S. Letokhov *Appl. Phys.* **24,** 89, (1981).
4. P. Lambropoulos, *Applied Optics* **19,** 3926, (1980).
5. J. P. Reilly and K. L. Kompa, *J. Chem. Phys.* **73,** 5468, (1980).
6. D. H. Parker, R. B. Bernstein and D. A. Lichtin, *J. Chem. Phys.* **75,** 2577, (1981).
7. For a recent concise discussion see: A. Gedanken, M. B. Robin and N. A. Kuebler, *J. Phys. Chem.* **86,** 4096, (1982).
8. D. P. Gerrity, L. J. Rothberg and V. Vaida, *Chem. Phys Lett.* **74,** 1 (1980).
9. G. J. Fisanick, A. Gedanken, T. S. Eichelberger, N. A. Kuebler and M. B. Robin, *J. Chem. Phys.* **75,** 5215; (1981).
10. J. Silberstein and R. D. Levine, *Chem. Phys. Lett.* **74,** 6, (1980).
11. (a) D. H. Russell, M. L. Gross, J. Van der Greef and N. M. M. Nibbering, *Org. Mass Spectrom.* **14,** 474 (1979); (b) D. H. Russell, M. L. Gross and N. M. M. Nibbering, *J. Am. Chem. Soc.* **100,** 6133, (1978).
12. F. Borchers, K. Levson, C. B. Theissling and N. M. M. Nibbering, *Org. Mass Spectrom.* **14,** 474, (1977).
13. A. Maquestiau, Y. V. Van Haverbeke, R. Flammang, C. De Meyes, K. B. Das, and G. S. Reddy, *Org. Mass Spectrom.* **12,** 631, (1977).
14. H. J. Walther, H. Eyer, U. P. Schlunegger, C. J. Porter, E. A. Larka and J. H. Beynon, *Org. Mass Spectrom.* **17,** 81, (1982).
15. R. S. Pandolfi, D. A. Gobeli and M. A. El-Sayed, *J. Phys. Chem.* **85,** 1779, (1981).
16. D. Proch, D. M. Rider and R. N. Zare, *Chem. Phys. Lett.* **81,** 430, (1981).
17. F. Rebentrost and A. Ben-Shaul, *J. Chem. Phys.* **74,** 3255 (1981).
18. J. L. Franklin, J. G. Dillard, H. M. Rosenstock, J. T. Herron, K. Draxl and F. H. Field, *Natl. Stand. Ref. Data Ser. Natl. Bur. Stand.* **26,** (1969).
19. T. P. Debies and J. W. Rabalais, *J. Electron Spectrosc.* **1,** 83, (1972).

20. Data for calculations were taken from Ref. 17 and the following sources: H. M. Rosenstock, K. Draxl, B. W. Steiner and J. T. Herron, *J. Phys. Chem. Ref. Data* **6,** Suppl. 1 (1977); G. Herzberg, *Molecular Spectra and Molecular Structure*, Vols. I–III (Van Nostrand, New York 1958); S. W. Benson, *Thermochemical Kinetics: Methods for the Estimation of Thermochemical Data and Rate Parameters* (John Wiley & Sons, New York, 1976); F. Rebentrost and A. Ben-Shaul, FORTRAN computer program forming basis for Ref. 17.
21. Jeng-Jiun Yang, F. Rebentrost and M. A. El-Sayed, in preparation.